Using a structural root system model for an in-depth assessment of root image analysis pipeline

Guillaume Lobet [1,2,*], Iko Koevoets [3], Pierre Tocquin[1],
Loïc Pagès[4] and Claire Périlleux[1]

[1] InBioS-PhytoSYSTEMS,
University of Liège, 4000 Liège, Belgium

[2] Institut fur Bio-und Geowissenschaften: Agrosphare,
Forschungszentrum Jülich, D52425 Jülich, Germany

[3] Plant Cell Biology, Swammerdam Institute for Life Sciences,
University of Amsterdam, 1098 XH Amsterdam, The Netherlands

[4] INRA, Centre d' Avignon, UR 1115 PSH,
Site Agroparc, 84914 Avignon cedex 9, France

* Corresponding author: g.lobet@fz-juelich.de

1   Abstract

2   Root system analysis is a complex task, often performed using fully automated image analysis

3   pipelines. However, these pipelines are usually evaluated with a limited number of ground-truthed

4   root images, most likely of limited size and complexity.

5

6   We have used a root model, ArchiSimple to create a large and diverse library of ground-truthed

7   root system images (10.000). This library was used to evaluate the accuracy and usefulness of

8   several image descriptors classicaly used in root image analysis pipelines.

9

10   Our analysis highlighted that the accuracy of the different metrics is strongly linked to the type of

11   root system analysed (e.g. dicot or monocot) as well as their size and complexity. Metrics that have

12   been shown to be accurate for small dicot root systems might fail for large dicots root systems or

13   small monocot root systems. Our study also demonstrated that the usefulness of the different

14   metrics when trying to discriminate genotypes or experimental conditions may vary.

15

16   Overall, our analysis is a call to caution when automatically analysing root images. If a thorough

17   calibration is not performed on the dataset of interest, unexpected errors might arise, especially for

18   large and complex root images. To facilitate such calibration, both the image library and the

19   different codes used in the study have been made available to the community.

20

Introduction

21

22   Roots are of outmost importance in the life of plants and hence selection on root systems

23   represents great promise for improving crop tolerance (as reviewed in (Koevoets et al., 2016)). As

24   such, their quantification is a challenge in a multitude of research projects. This quantification is

25   usually twofold. The first step consists in acquiring an image of the root system, either using classic

26   image techniques (CCD cameras) or more specialized ones (microCT, X-Ray, fluorescence, ...). The

27   next step is to analyse the picture in order to extract meaningful descriptors of the root system.

28

29   To paraphrase the famous belgian surrealist painter, René Magritte, figure 1A is not a root system.

30   Figure 1A is an image of a root system and that distinction is important. Such an image is indeed a

31   two dimensional representation of a root system, which is usually a three dimensional object. Until

32   now, measurements are generally not performed on the root systems themselves, but on the images

33   and this raises some issues.

34

35   Image analysis is, by definition, the obtention of metrics (or descriptors) describing the objects

36   contained in a particular image . In a perfect situation, these descriptors would accurately represent

37   the biological object of the image with negligible deviation from the biological truth (or data).

38   However, in many cases, artefacts might be present in the images so that the representation of the

39   biological object is not accurate anymore. These artefacts might be due to the conditions in which

40   the images were taken or to the object itself. Mature root systems, for instance, are complex

41   branched structure, composed of thousands of overlapping (fig. 1B) and crossing linear segments

42   (fig. 1C). These features are likely to impede image analysis and create a gap between the

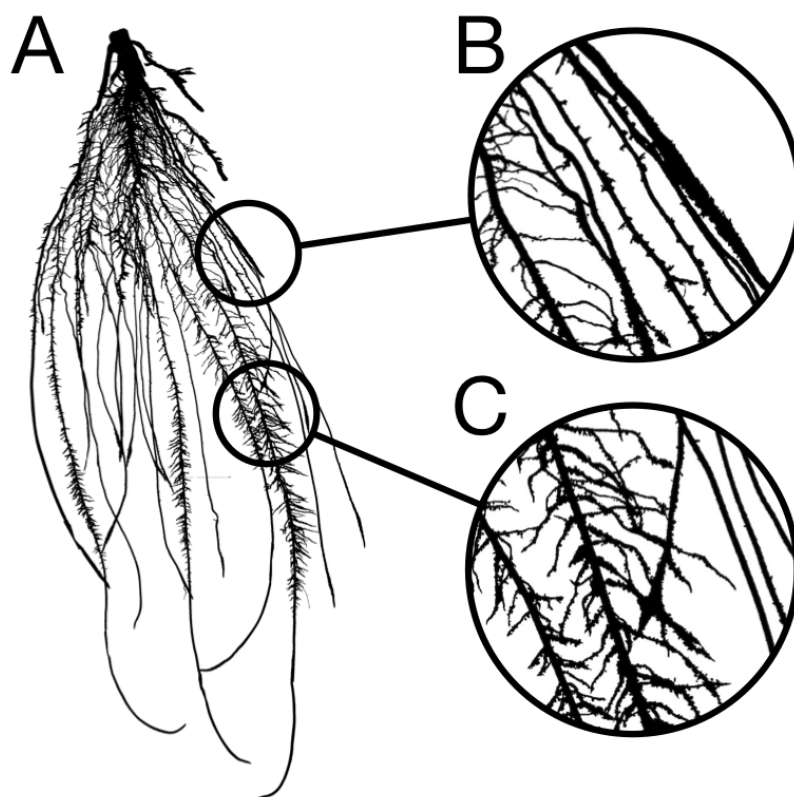43   descriptors and the data.

44

Figure 1. A. Image of a 2-week old maize root system grown in rhizotron. **B.** Close-up showing overlapping roots. **C.** Close-up showing crossing roots.

45

46

47   Root image descriptors can be separated into two main categories: morphological and geometrical

48   descriptors. Morphological descriptors refer to the shape of the different root segments forming the

49   root system (table 1). They include, among others, the length and diameter of the different roots.

50   For complex root system images, morphological descriptors are difficult to obtain and are prone to

51   error as mentioned above.

52

53   Geometrical descriptors give the position of the different root segments in space. They summarize

54   the shape of the root system as a whole. The simplest geometrical descriptors are the width and

55   depth of the root system. Since these descriptors are mostly defined by the outside envelope of the

56 root system, crossing and overlapping roots have little impact on their estimation and they can be

57 considered as relatively errorless. Geometrical descriptors are expected to be loosely linked to the

58 actual root system topology, as identical shapes could be reached by different root systems (the

59 opposite is true as well). They are usually used in genetic studies, to identify genetic bases of root

60 system shape and soil exploration.

61

62 Several automated analysis tools were designed in the last few years to extract both type of

63 descriptors from root images (Armengaud et al., 2009; Bucksch et al., 2014; Galkovskyi et al., 2012;

64 Pierret et al., 2013). However, the validation of such tools is often incomplete and/or error prone.

65 Indeed, for technical reasons, the validation is usually performed on a small number of ground-

66 truthed images of young root systems for which most analysis tools were actually designed . In the

67 few cases where validation is performed on large and complex root systems, it is usually not on

68 ground-truthed images, but in comparison with previously published tools (measurement of X with

69 tool A compared with the same measurement with tool B). This might seem reasonable approach

70 regarding the scarcity of ground-truthed images of large root systems. However, the inherent

71 limitations of these tools, such as scale or plant type (monocot, dicot) are often not known. Users

72 might not even be aware that such limitations exist and apply the provided algorithm without

73 further validation on their own images. This can lead to unsuspected errors in the final

74 measurements.

75

76 One strategy to address the lack of in-depth validation of image analysis pipeline would be to use

77 synthetic images generated by structural root models (models designed to recreate the physical

78 structure and shape of root systems). Many structural root models have been developed, either to

79 model specific plant species (Pagès et al., 1989), or to be generic (Pagès et al., 2004; 2013). These

80 models have been repeatedly shown to faithfully represent the root system structure (Pagès and

81   Pellerin, 1996). In addition, they can provide the ground-truth data for each synthetic root system

82   generated, independently of its complexity. However, except one recent tool designed for young

83   seedlings with no lateral roots (Benoit et al., 2014). they have almost never been used for validation

84   of image analysis tools (Rellán-Álvarez et al., 2015). A

85

86   Here we (i) illustrate the use of a structural root model, Archisimple, to systematically analyse and

87   evaluate an image analysis pipeline and (ii) evaluate the usefulness of different root metrics

88   commonly used in plant root research.

89

Material and methods

Nomenclature used in the paper

Ground-truth data: The real (geometric and morphometric) properties of the root system as a biological object. Determined by either manual tracing of roots or by using the output of modelled root systems.

(Image) Descriptor: Property of the root image. Does not necessarily have a biological meaning.

Synthetype: For each simulation, a parameter set is defined randomly. Then, 10 root systems are created. Since the model has an intrinsic variability, each of these root system is slightly different from the others, although similar, forming what we called a synthetic genotype, or *synthetype*.

Root axes: first order roots, directly attached to the shoot

Lateral root: second (or lower) order roots, attached to an other root

Creation of a root system library

We used the model ArchiSimple, which was shown to allow generating a large diversity of root systems with a minimal amount of parameters (Pagès et al., 2013). In order to produce a large library of root systems , we ran the model 10.000 times, each time with a random set of parameters.

The simulations were divided in two main groups: monocots and dicots. For the monocot simulations, the model generated a random number of first-order axes and secondary (radial) growth was disabled. For dicot simulations, only one primary axis was produced and secondary

110   growth was enabled (the extend of which was determined by a random parameter) . For all

111   simulation, only first order laterals were created, to limit complexity.

112

113   The root system created from each simulation was stored in an RSML file. Each RSML file was then

114   read by the RSML Reader plugin from ImageJ to extract metrics and generate ground-truth data for

115   the library (Lobet et al., 2015). These ground-truth data included geometrical,morphological and

116   topological parameters (table 1). For each RSML data file, the RSML Reader plugin also created a

117   PNG image (at a resolution of 300 DPI) of the root system.

118

119   **Table 1:** Root system parameters used as ground-truth data

Name	Description	Unit
tot_root_length	The cumulative length of all roots	mm
tot_prim_length	The cumulative length of all root axes	mm
tot_lat_length	The cumulative length of all lateral roots	mm
mean_prim_length	The mean first-order roots length	mm
mean_lat_length	The mean lateral root length	mm
n_primary	The total number of first order roots	-
n_laterals	The total number of lateral roots	-
mean_lat_density	The mean lateral root density: for each first-orde root, the number of lateral roots divided by the axis length (total length).	mm-1
mean_prim_diam	The mean diameter of the first-order roots	mm
mean_lat_diam	The mean diameter of the lateral roots	mm
mean_lat_angle	The mean insertion angle of the lateral roots	°

120

Root image analysis

122   Each generated image was analysed using a custom-made ImageJ plugin, Root Image Analysis-J (or

123   RIA-J). The source code of RIA-J, as well as a compiled version is available at the address:

124   https://zenodo.org/record/61509.

125

126   For each image, we extracted a set of classical root image descriptors, such as the total root length,

127   the projected area or the number of visible root tips. In addition, we included shape descriptors,

128   such as pseudo-landmarks, or a-dimensional metrics such as the exploration ratio, of the width

129   proportion at 50% depth (see Supplemental file 1 for details about the shape descriptors). The list

130   of metrics and algorithms used by our pipeline is listed in the table 2.

Data analysis

132   Data analysis was performed in R (R Core Team). Morphometric analyses were performed using the

133   *momocs* (Bonhomme et al., 2014) and *shapes* (Dryden, 2015)packages. Plots were created using

134   *ggplot2* (Wickham, 2009) and *lattice* (Sarkar, 2008).

135   The Relative Root Square Mean Errors (RRSME) were estimated using the equation:

$$RRMSE = \sqrt{\frac{\sum^n \frac{(\overline{yi} - yi)}{\overline{yi}}}{n}}$$

136   where n is the number of observations, $\overline{yi}$ is the mean and yi is the estimated mean.

137   The Linear Discriminant Analysis (LDA) was performed using the *lda* function from the *MASS*

138   package (M and D, 2002). For each analysis, we used the *synthetyp*e information as grouping factor.

139   We used half of the samples (5) of each *synthetype* to build the model and the other half to assess

140   the discriminant power of the each class of metrics (morphology and shape).

9

141 # Data availability

142   All data used in this paper (including the image and RSML libraries) are available at the address

143   https://zenodo.org/record/61739

144   An archived version of the codes used in this paper is available at the address

145   https://zenodo.org/record/152083

146

Results and discussions

Production of a large library of ground-truthed root system images

149 We combined existing tools into a single pipeline to produce a large library of ground-truthed root

150 system images. The pipeline combines a root model (ArchiSimple (Pagès et al., 2013)), the Root

151 System Markup Language (RSML) and the RSML Reader plugin from ImageJ (Lobet et al., 2015). In

152 short, ArchiSimple was used to create a large number of root systems, based on random input

153 parameter sets. Each output was stored as an RSML file (fig. 2A), which was then used by the RSML

154 Reader plugin to create a graphical representation of the root system (as a .jpeg file) and a ground-

155 truth dataset (fig. 2B). Details about the different steps are presented in the Materials and Methods
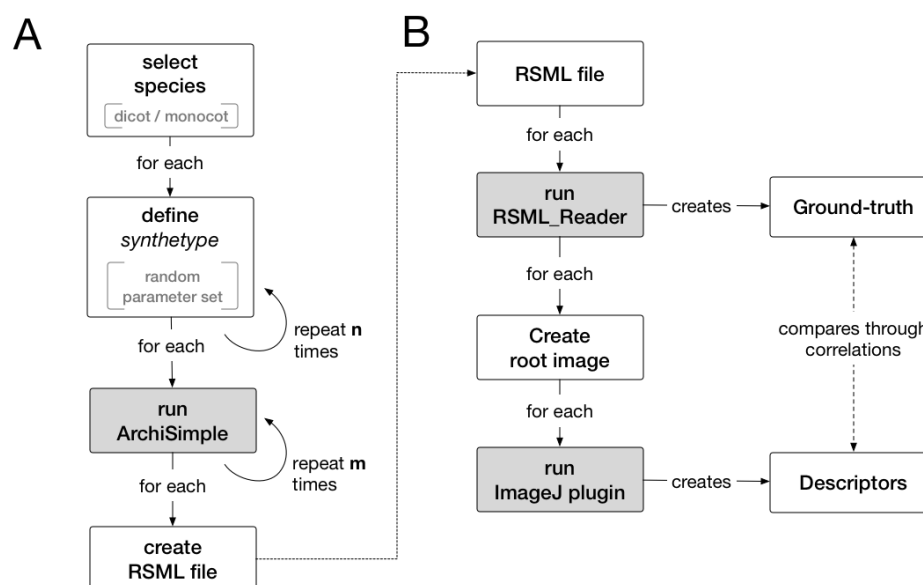
156 section.

Figure 2: Overview of the workflow used in this study. **A.** Generation of root systems using ArchiSimple. **B.** Creation and analysis of root images.

159   We used the pipeline to create a library of 10,000 root system images, separated into monocots

160   (multiple first order roots and no secondary growth) and dicots (one first order root and secondary

161   growth). For each input parameter-set used for ArchiSimple (1.000 different ones), 10 repetitions

162   were performed to create *synthetic genotypes*, or *synthetypes* (fig. 2A). The synthetype repetitions

163   were done such as the structure of the final dataset would mimic the structure of a dataset

164   containing phenotypic data of different genotypes. The ranges of the different ground-truth data are

165   shown in table 2 and their distribution is shown in the Supplemental Figure 1. The pipeline

166   produced perfectly thresholded black and white images and hence the following analyses were

167   focused on the characterisation of the root objects themselves.

168

169   We started by evaluating whether monocots and dicots should be separated during the analysis. We

170   performed a Principal Component Analysis on the ground-truthed dataset to assess if the *species*

171   grouping had an effect on the overall dataset structure (fig. 3A). Monocots and dicots formed

172   distinct groups (MANOVA p-value < 0.001), with only minimal overlap. The first principal

173   component, that represented 33.2% of the variation within the dataset, was mostly influenced by

174   the number of primary axes. The second principal component (19.6% of the variation) was

175   influenced, in part, by the root diameters. These two effects were consistent with the clear grouping

176   of monocots and dicots, since they expressed the main difference between the two *species*.

177   Therefore, since the *species* grouping had such a strong effect on the overall structure, we decided

178   to analyse them separately rather than together for the following analyses.

179

180 **Table 3:** Ranges of the different ground-truth data from the root systems generated using

181 ArchiSimple

| variable	minimum value	maximum value	unit
MONOCOTS			
tot_root_length	8.36	2455.03	cm
width	0.25	33.21	cm
depth	5.49	37.5	cm
n_primary	1	20	-
tot_prim_length	6	327	cm
mean_prim_length	3.22	38	cm
mean_prim_diameter	0.02	0.04	cm
mean_lat_density	0	100.88	cm
n_laterals	0	1378	-
tot_lat_length	0	1630	cm
mean_lat_length	0	4.44	cm
mean_lat_diameter	0	0.03	cm
mean_lat_angle	0	97.74	°
DICOTS			
tot_root_length	6.91	585.05	cm
width	0.01	15.05	cm
depth	3.89	36.99	cm
n_primary	1	1	-
tot_prim_length	4	37	cm
mean_prim_length	4.4	37.5	cm
mean_prim_diameter	0.02	1.13	cm
mean_lat_density	0	494.54	cm
n_laterals	0	277	-
tot_lat_length	0	437	cm
mean_lat_length	0	5.48	cm
mean_lat_diameter	0	0.23	cm
mean_lat_angle	0	87.63	°

182
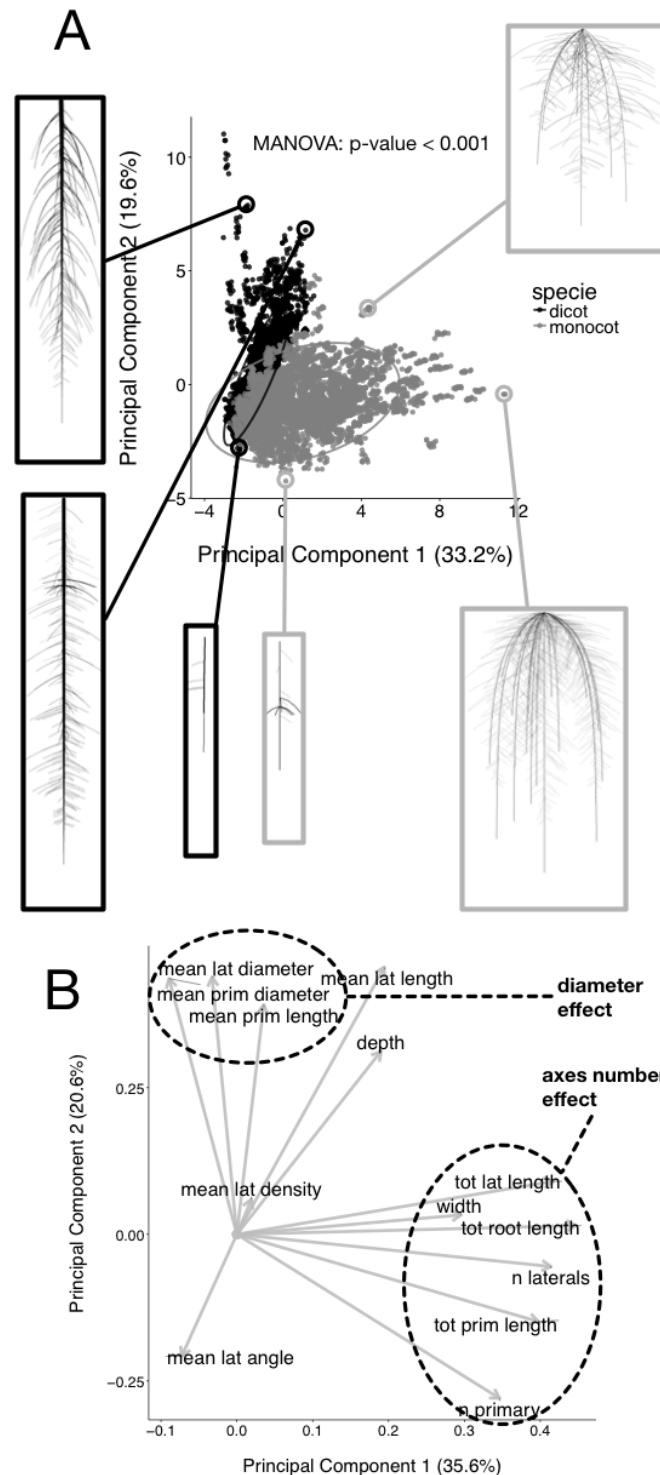
Figure 3: A. Principal Component Analysis of the root ground-truth dataset. Images of the selected root systems have been added for illustration. **B.** Loadings of the Principal Component Analysis.

183

Systematic evaluation of root image descriptors

184

185 In order to demonstrate the utility of a synthetic library of ground-truthed root systems, we

186 analysed every image of the library using a custom-built root image analysis tool, RIA-J. We decided

187 to do so because our purpose was to test the usefulness of the synthetic analysis and not to assess

188 the accuracy of existing tools. Nonetheless, RIA-J was designed using known and published

189 algorithms, often used in root system quantification. A detailed description of RIA-J can be found in

190 the Materials and Methods section.

191

192 **Table 3:** Root image descriptors extracted by RIA-J

Name	Description	Unit	Reference
area	Projected area of the root system	mm^2	(Galkovskyi et al., 2012)
length	Length of the skeleton of the root system image	mm	(Galkovskyi et al., 2012)
tip_count	Number of end branches in the root system skeleton	-	
diam_mean	Mean diameter of the root object in the image	mm	
width	The maximal width of the root system	mm	-
depth	The maximal depth of the root system	mm	-
width_depth	Ratio between the width and the depth of the root system	-	(Galkovskyi et al., 2012)
com_x - com_y	Relative coordinates of the center of mass of the root system	-	(Galkovskyi et al., 2012)
convexhull	Area of the smallest convex shape around the root system	mm^2	(Galkovskyi et al., 2012)
exploration	Ratio between the convex hull area and the projected area	-	(Galkovskyi et al., 2012)
PL.PC1-3	First three Principal Components of the morphometric analysis using pseudo-landmarks (see Supplemental file 1 for details)	-	(Chitwood and Otoni, 2016; Rellán-Álvarez et al., 2015; Ristova et al., 2013)
width50	Relative depth at which 50% of the cumulative width of the root system is reached (see Supplemental file 1 for details)	-	(Bucksch et al., 2014)
count50	Relative depth at which 50% of the total number of roots is reached	-	(Bucksch et al., 2014)

193

194   We extracted 16 descriptors from each root system image (Table 3) and compared them with their

195   own ground-truth data. For each pair of descriptor/data, we performed a linear regression and

196   computed its r-squared value. Figure 4 shows the results from the different combinations for both

197   monocots and dicots. We can observe that, as a general rule, good correlations were rare, with only

198   3% of the combinations having an r-squared above 0.8. In addition, even a good correlation is not

199   necessarily directly useful as the relationship between the two variables might not follow a 1:1 rule

200   (fig. 4B-C). In such case, an additional validation might be needed to define the relation between

201   both variables.

202

203   It also has to be noted that the correlations were different between species. As an example, within

204   the dicot dataset, no good correlation was found between the *tip_count* and *diam_mean* estimators

205   while better correlation was found for the monocots. As a consequence, validation of the different

206   image analysis algorithms should be performed, at least, for each group of species. An algorithm

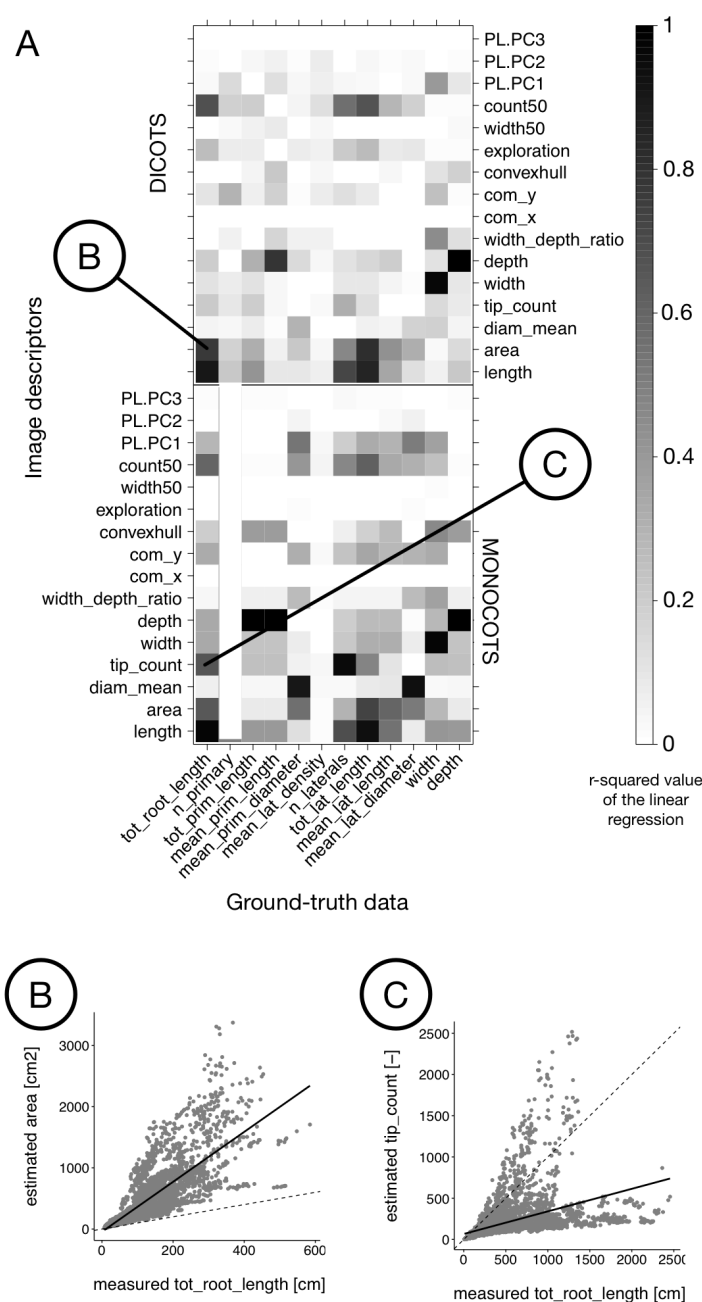207   giving good results for a monocot might fail when applied on dicot root system analysis.

Figure 4: A. Heatmap of the r-squared values between the different image descriptors and the ground-truth values. Black represents an r-squared value of 1; white represents a value of 0. Upper panel: dicot dataset. Lower panel: monocot dataset. **B & C**. Details of the regressions. The plain black line represent the fitted regressions while the dotted line represents the 1:1 relationship.

208

17

209 Errors from image descriptors are likely to be non linear

210   In addition to being related to the species of study, estimation errors are likely to increase with the

211   root system size. As the root system grows and develops, the crossing and overlapping segments

212   increase, making the subsequent image analysis potentially more difficult and prone to error.

213   However, a systematic analysis of such error is seldom performed.

214

215   Figure 5 shows the relationship between the ground-truth and descriptor values for three

216   parameters: the total root length (fig. 5A), the number of roots (fig. 5B) and the root system depth

217   (fig. 5C). For each of these variables, we quantified the Relative Root Mean Square Error (see

218   Materials and Methods for details) as a function of the total root length. We can observe that for the

219   estimation of both the total root length and the number of lateral roots, the Relative Root Square

220   Mean Error increased with the size of the root system (fig. 5A-B). As stated above, such increase of

221   the error was somehow expected with increasing complexity. For other metrics, such as the root

222   system depth, no errors were expected (*depth* is supposedly an error-less variable) and the Relative

223   Root Mean Square Error was close to 0 whatever the size of the root system.

224

225   Such results are a call to caution when analysing root images as unexpected errors in descriptors

226   estimation can arise. This is probably even more true with real images, that are susceptible to

227   contain non-root objects (e.g. dirt) and lower order laterals roots (as stated above, simulations used

228   here were limited to first order laterals).
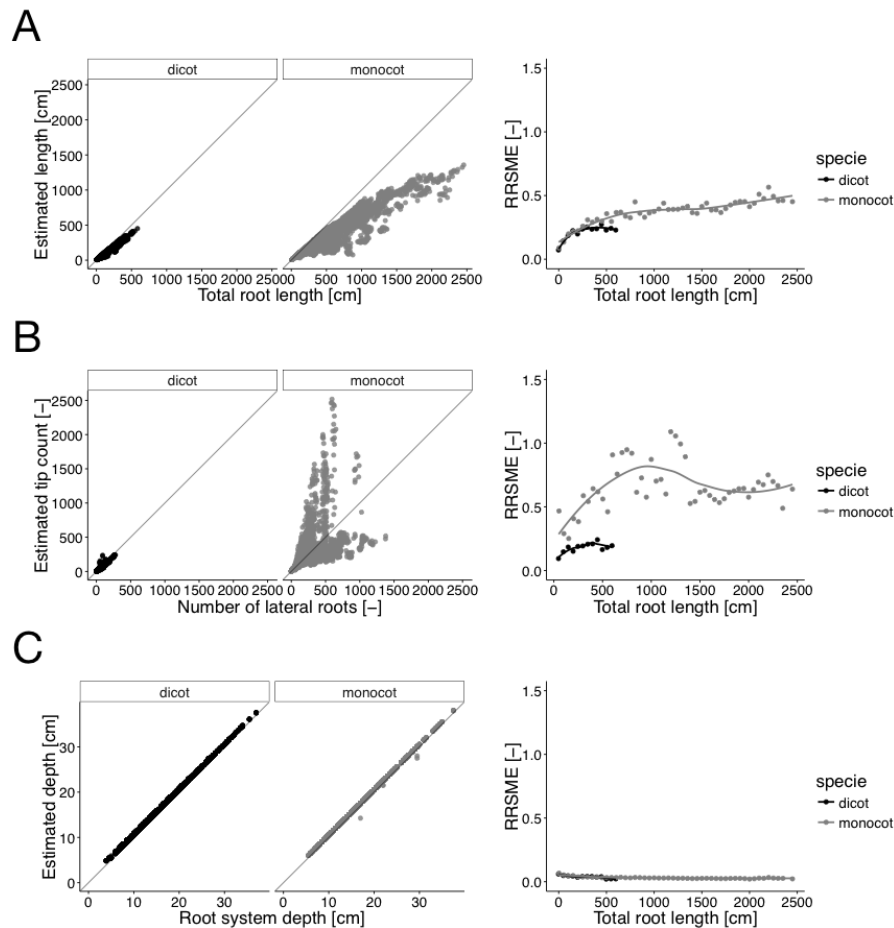
18

Figure 5: Error estimation for three ground-truth parameters. Left panel shows the relationship between the descriptors and the corresponding ground-truth variables. Right panels show the evolution of the Relative Root Mean Square Error (RRSME) as a function of the ground-truth variable. For the RRSME calculations, the continuous variables were discretised in groups. **A**. Total root length. **B.** Number of lateral roots. **C.** Root system depth

229

230

231

232 Differentiation power differs between metrics

233 Finally, we wanted to evaluate which metrics were the most useful to discriminate between root

234 systems of different genotypes or experimental series (control vs treatment). As explained above,

235 for each parameter set used in the ArchiSimple run for library construction, we generated 10 root

236 systems. Given the intrinsic variability existing in the model, each of these 10 root systems were

237 similar although different, as could be expected from plants of the same genotype. These so-called

238 *synthetypes*, were then used to evaluate how efficient were the different metrics to discriminate

239 them.

240

241 To estimate the differentiation of the image metrics, we used a Linear Discriminant Analysis (LDA)

242 prediction model. For each synthetype, half of the plants were used to create the LDA model. The

243 model was then used to predict a synthetype for the remaining half of the plants. This approach

244 allowed us to evaluate the prediction accuracy, or differentiation power, of the different metrics. A

245 prediction accuracy of 100% means that all plants were correctly assigned to their synthetype. To

246 evaluate the differentiation power of single metrics, we used an approach in which each metric was

247 iteratively added to the model, based on the model global prediction power (see Supplemental

248 Figure 3 for details about the procedure) . We performed the analysis either on a full dataset (fig.

249 6D-E), or on a data restrictedto the smallest plants (fig. 6A), in order to test the influence of the

250 underlying data structure.

251

252 Two main observations can be made on the figure 6. First, for three out of four scenarios, only 5 (or

253 less) descriptors were needed to achieve a differentiation accuracy of 90%. *Depth*, *area* and *length*

254 were the most important descriptors in almost all scenarios. The remaining descriptors did not

255 increase significantly the accuracy (some might even decrease it). This might be interpreted as a

256   handful of variables were sufficient to distinguish *synthetypes*, and by extension genotypes or

257   treated plants. However, we can also observe that the most important parameters changed

258   depending on the underlying data structure (either due to species or the size of the dataset). This

259   indicates that it is difficult to have an *a priori* evaluation of the important variables. Keeping as

260   many variable a possible might always be the most efficient solution.
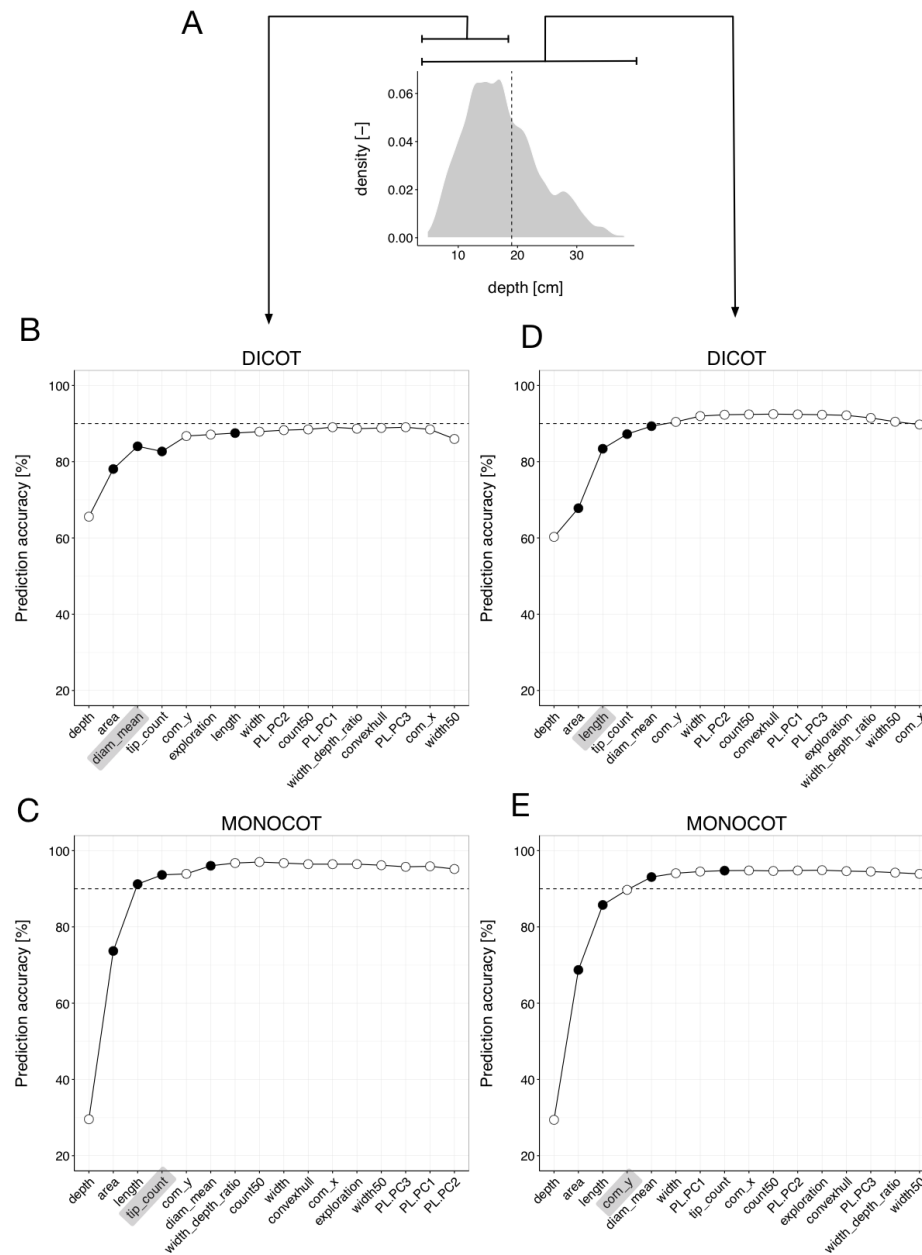
261

Figure 6: A. Distribution of the simulated root system depths. The dotted line represent the threshold used to generate a partial dataset. **B-E**. Evaluation of the differentiation power of the different image metrics. Each point corresponds to the prediction accuracy of the Linear Discriminant Analysis model, with an increasing number of metrics included. The abscise axis represents the variables iteratively added to the model. **B-C.** Prediction accuracy for a partial dataset. **D-E:** Prediction accuracy for the full dataset. **B-D:** Dicots. **C-E:** Monocots. Empty dots represent morphological metrics. Plain dots represent geometrical metrics. The dotted line represent the 90% precision accuracy threshold.

262

Conclusions

263

264   The automated analysis of root system images is routinely performed in many research projects.

265   Here we used a library of 10.000 modelled images to estimate the accuracy and usefulness of

266   different image descriptors extracted with an home-made root image analysis pipeline. The analysis

267   highlighted some important limitations during the image analysis process.

268

269   Firstly, general structure of the root system (e.g monocot vs dicots) can have a strong influence on

270   the descriptors accuracy. Descriptors that have been shown to be good predictors for one type of

271   root systems might fail for another type. In some cases, the calibration and the combination of

272   different descriptors might improve the accuracy of the predictions, but this needs to be assessed

273   for each analysis.

274

275   A second factor influencing strongly the accuracy of the analysis is the root system size and

276   complexity. As a general rule, for morphological descriptors, the larger the root system, the larger

277   the error is. So far, a large proportion of the root research has been focused on seedlings with small

278   root systems and have *de facto* avoided such errors. However, as the research questions are likely

279   to focus more on mature root system in the future, these limitations will become critical.

280

281   Finally we have shown that not all metrics have the same benefit when comparing genotype or

282   treatments. Again, depending on the root system type or size, different metrics will have different

283   differentiation powers.

284

285   It is important to highlight that the images used in our analysis were perfectly thresholded, without

286   any degradation in the image quality. Therefore, the errors computed in our analysis are likely

23

287   under-estimated compared to real images (with additional background noise and lesser quality).

288   Since the quality of the images is dependent on the underlying experimental setup, artificial noise

289   could be added to the generated images in order to mimic any experimentally induced artifact and

290   to improve the analysis pipeline evaluation, as proposed by (Benoit et al., 2014).

291

292   To conclude, our study is a reminder that thorough calibrations are needed for root image analysis

293   pipelines. Here we have used a large library of simulated root images, that we hope will be helpful

294   for the root research community to evaluate current and future image analysis pipelines.

295

296

Conflict of Interest

297

The authors declare that the research was conducted in the absence of any commercial or financial

298

relationships that could be construed as a potential conflict of interest.

299

Author Contributions

300

GL, LP, PT and CP designed the study. IK developed the image analysis pipeline RIA-J. GL generated

301

the image library, did the image analysis and data analysis. LP developed the ArchiSimple model. All

302

authors have participated in the writing of the manuscript.

303

Funding

304

Supplementary Material

308

- **Supplemental figure 1:**   Distribution of the properties of the modelled root images

309

- **Supplemental figure 2:** Distribution of the descriptors of the modelled root images

310

- **Supplemental figure 3:** Workflow used for the accuracy analysis

311

- **Supplemental file 1:** Defintions of the shape descriptors

312

313

314 References

315 Armengaud, P., Zambaux, P., Hills, A., Sulpice, R., Pattison, R. J., Blatt, M. R., et al. (2009). EZ-Rhizo: integrated
316   software for the fast and accurate measurement of root system architecture. *Plant J* 57, 945–956.

317 Benoit, L., Rousseau, D., Belin, É., Demilly, D., and Chapeau-Blondeau, F. (2014). Simulation of image
318   acquisition in machine vision dedicated to seedling elongation to validate image processing root
319   segmentation algorithms. *Computers and Electronics in Agriculture* 104, 84–92.
320   doi:10.1016/j.compag.2014.04.001.

321 Bonhomme, V., Picq, S., and Gaucherel, C. (2014). Momocs: outline analysis using R. *Journal of Statistical ….*

322 Bucksch, A., Burridge, J., York, L. M., Das, A., Nord, E., Weitz, J. S., et al. (2014). Image-based high-throughput
323   field phenotyping of crop roots. doi:10.1104/pp.114.243519.

324 Chitwood, D. H., and Otoni, W. C. (2016). Morphometric analysis of Passiflora leaves I: the relationship
325   between landmarks of the vasculature and elliptical Fourier descriptors of the blade.
326   doi:10.1101/067512.

327 Dryden, I. L. (2015). shapes package. Vienna, Austria.

328 Galkovskyi, T., Mileyko, Y., Bucksch, A., Moore, B., Symonova, O., Price, C. A., et al. (2012). GiA Roots: software
329   for the high throughput analysis of plant root system architecture. *BMC Plant Biol* 12, 116.
330   doi:10.1186/1471-2229-12-116.

331 Koevoets, I. T., Venema, J. H., Elzenga, J. T. M., and Testerink, C. (2016). Roots Withstanding their
332   Environment: Exploiting Root System Architecture Responses to Abiotic Stress to Improve Crop
333   Tolerance. *Front Plant Sci* 07, 91–19. doi:10.3389/fpls.2016.01335.

334 Lobet, G., Pound, M. P., Diener, J., Pradal, C., Draye, X., Godin, C., et al. (2015). Root System Markup Language:
335   Toward a Unified Root Architecture Description Language. *Plant Physiol* 167, 617–627.
336   doi:10.1104/pp.114.253625.

337 M, V. W., and D, R. B. (2002). *Modern Applied Statistics with S*

338 . New-York: Springer.

339 Pagès, L., and Pellerin, S. (1996). Study of differences between vertical root maps observed in a maize crop
340   and simulated maps obtained using a model for the three-dimensional architecture of the root system.
341   *Plant and Soil* 182, 329–337.

342   Pagès, L., Bécel, C., Boukcim, H., Moreau, D., Nguyen, C., and Voisin, A.-S. (2013). Calibration and evaluation of
343   ArchiSimple, a simple model of root system architecture. *Ecological Modelling* 290, 76–84.
344   doi:10.1016/j.ecolmodel.2013.11.014.

345   Pagès, L., Jordan, M. O., and Picard, D. (1989). A simulation model of the three-dimensional architecture of the
346   maize root system. *Plant and Soil* 119, 147–154. doi:10.1007/BF02370279.

347   Pagès, L., Vercambre, G., Drouet, J.-L., Lecompte, F., Collet, C., and LeBot, J. (2004). RootTyp: a generic model
348   to depict and analyse the root system architecture. *Plant and Soil* 258, 103–119.

349   Pierret, A., Gonkhamdee, S., Jourdan, C., and Maeght, J.-L. (2013). IJ-Rhizo: an open-source software to
350   measure scanned images of root samples. *Plant and Soil*, 1–9. doi:10.1007/s11104-013-1795-9.

351   R Core Team R: A Language and Environment for Statistical Computing.

352   Rellán-Álvarez, R., Lobet, G., Lindner, H., Pradier, P.-L., Sebastian, J., Yee, M.-C., et al. (2015). GLO-Roots: an
353   imaging platform enabling multidimensional characterization of soil-grown root systems. *eLife* 4,
354   e07597. doi:10.7554/eLife.07597.

355   Ristova, D., Rosas, U., Krouk, G., Ruffel, S., Birnbaum, K. D., and Coruzzi, G. M. (2013). RootScape: A landmark-
356   based system for rapid screening of root architecture in Arabidopsis thaliana.
357   doi:10.1104/pp.112.210872.

358   Sarkar, D. (2008). *Lattice: Multivariate Data Visualization with R*. New York: Springer.

359   Wickham, H. (2009). *ggplot2*. New York, NY: Springer New York doi:10.1007/978-0-387-98141-3.

360